Available online at www.sciencedirect.com
SCIENCE DIRECT®
ELSEVIER
International Journal of Solids and Structures 43 (2006) 2710–2722
INTERNATIONAL JOURNAL OF SOLIDS and STRUCTURES
www.elsevier.com/locate/ijsolstr

The stress intensities of three-dimensional corner singularities in a laminated composite

Yongwoo Lee [a], Insu Jeon [b,*], Seyoung Im [a]

[a] *Department of Mechanical Engineering, Korea Advanced Institute of Science and Technology (KAIST), Science Town, Daejeon 305-701, Republic of Korea*
[b] *Materials Research Institute for Sustainable Development, National Institute of Advanced Industrial Science and Technology (AIST), 2266-98 Anagahora, Shimoshidami, Moriyama-ku, Nagoya 463-8560, Japan*

Received 21 January 2005; received in revised form 20 June 2005
Available online 24 August 2005

Abstract

The stress intensity of three-dimensional corner singularity is computed for the tip of a transverse crack terminating on the free surface in a laminated composite. Firstly, stress singularity is calculated via finite element method applied for the angular domain. Then the two-state M-integral is employed, in conjunction with eigenfunction expansion, for computing the stress intensity of the stress singularity. The numerical example demonstrates the effectiveness of the proposed computational scheme.

Keywords: Three-dimensional corner singularity; Transverse crack; Laminated composite; Stress intensity; Conservation integrals

1. Introduction

The determination of stress intensities as well as the stress singularities of singular stress fields around generic wedges in linear elastic materials has been a major subject in fracture mechanics. In three-dimensional wedges, however, most works did not look into the near-tip stress intensities of the singular stress field, but concentrated on calculating only the stress singularities. This is partly because three-dimensional problems are themselves very complicated and partly because any reliable methodology to compute stress intensities or a fracture parameter like the J-integral for three-dimensional cracks was not available.

* Corresponding author. Tel.: +81 52 736 7449; fax: +81 52 736 7400.
E-mail address: insu-jeon@aist.go.jp (I. Jeon).

0020-7683/$ - see front matter © 2005 Elsevier Ltd. All rights reserved.
doi:10.1016/j.ijsolstr.2005.06.050

There are many researchers that have discussed the order of stress singularities on three-dimensional wedge vertices. For example, Koguchi and Muramoto (2000), Picu and Gupta (1997), Ghahremani (1991), Somaratna and Ting (1986), Bazant and Estenssoro (1979), Benthem (1980, 1977) and others cited in these papers. Only a few studies have tried to compute the stress intensities as well as the stress singularities. For example, near the vertex of a thin plate with a crack, Nakamura and Parks (1989, 1988) introduced the corner stress intensity which is computed from the three-dimensional local J-integral. However, this method is applicable only for three-dimensional cracks. Labossiere and Dunn (2001) conducted a series of very elaborate testing to confirm that the near-tip stress intensities of the singular fields on the bimaterial free edges are accurately correlated to the initiation of fractures in the specimens. Furthermore, they showed that the intensities of the singular stresses around the three-dimensional wedge on the interface corner of the two joining materials are in an excellent correlation with the initiation of the failure at the wedge vertices of the specimens. Hence, of paramount importance is an efficient and accurate calculation of these near-tip intensities. Recently Lee and Im (2003) proposed a systematic computational scheme, which is a method to calculate the near-tip intensities of the singular stress fields around the three-dimensional wedges with the aid of the two-state M-integral.

The computation of the near-tip intensities of the singular fields may be rather straightforward for the two-dimensional wedges, and there are many schemes available (see Im and Kim, 2000 and the papers cited therein, for examples). Among others, the application of the two-state conservation integral (Im and Kim, 2000; Kim et al., 2001; Jeon and Im, 2001; Lee et al., 2001) is known to be a robust method of computation. Moreover, Lee and Im (2003) showed that the computational scheme using the two-state M-integral is applicable for three-dimensional wedges by computing the near-tip intensities for the vertex of a thick plate with a crack, and the bimaterial interface corner, which was considered by Labossiere and Dunn (2001).

The purpose of the present paper is to extend the computation of the near-tip intensities around three-dimensional wedges reported in our previous work (Lee and Im, 2003) to the case of anisotropic materials. A particular emphasis is given to the extension of the approach to the case of the three-dimensional crack corner of a laminated composite with transverse cracks or on the intersection of transverse cracks with free surface in composite laminates, which was treated by Somaratna and Ting (1986) and Ghahremani (1991). A brief review is first stated for the eigenfunction expansion of the solution for three-dimensional elastic wedges. This is followed by a summary regarding the two-state M-integral. The two-state M-integral is then applied for calculating the near-tip intensity by utilizing the complementarity relationship for the eigenvalues of the three-dimensional wedges. That is, the path or surface independence property of the two-state M-integral for a pair of the complementary eigenvalues is exploited to equate its value calculated on the vanishing near-field surface around the vertex to the value from finite element analysis on the far-field surface. This procedure enables us to calculate the intensity of the singular stress field around the wedge vertex in an efficient manner.

For the numerical example, we choose a crack corner of a laminated composite with transverse cracks, of which the stress singularities were discussed by Ghahremani (1991), and Somaratna and Ting (1986). This example demonstrates the effectiveness and accuracy of the proposed-scheme.

2. Eigenfunction expansion of the solution for three-dimensional elastic wedges

Let the stress and strain components in the spherical coordinates be represented by 1-D arrays as follows:

$$(\sigma_1, \sigma_2, \sigma_3, \sigma_4, \sigma_5, \sigma_6) = (\sigma_{rr}, \sigma_{\theta\theta}, \sigma_{\phi\phi}, \sigma_{\theta\phi}, \sigma_{r\phi}, \sigma_{r\theta}) \tag{1a}$$

$$(\varepsilon_1, \varepsilon_2, \varepsilon_3, \varepsilon_4, \varepsilon_5, \varepsilon_6) = (\varepsilon_{rr}, \varepsilon_{\theta\theta}, \varepsilon_{\phi\phi}, 2\varepsilon_{\theta\phi}, 2\varepsilon_{r\phi}, 2\varepsilon_{r\theta}) \tag{1b}$$

The material constitutive relationship is then given as

$$\sigma_i = C_{ij}\varepsilon_j$$

where $i,j = 1$–6, and C_{ij} is the material stiffness which satisfies $C_{ij} = C_{ji}$.

Consider a conical region V, which has its vertex O, the lateral boundary S_L, and the far-field boundary S_F, as shown in Fig. 1. The surface S_F may be subjected to a traction or displacement boundary condition, but the lateral surface S_L is free from traction, or subjected to a fixed rigid fixture constraining the displacements to be zero. This represents generic three-dimensional wedges or notches, and the typical examples include a three-dimensional crack-tip corner created at the intersection vertex between a crack front line and a free surface, and a three-dimensional bimaterial corner, which is formed by two intersecting free edges.

For the purpose of analysis for stress singularities at the vertex O, we introduce the eigenfunction expansion (Bazant and Estenssoro, 1979; Benthem, 1977; Lee and Im, 2003) for the elastic solution, of which displacements are zero at the vertex and differentiable in the domain. The displacement fields near the vertex are given in the separable form as

$$\begin{aligned} u &= \frac{1}{2\mu}\mathrm{Re}\left[\sum_{\delta_n}\beta_n r^{\delta_n+1}\tilde{u}_n(\theta,\phi;\delta_n)\right] \\ v &= \frac{1}{2\mu}\mathrm{Re}\left[\sum_{\delta_n}\beta_n r^{\delta_n+1}\tilde{v}_n(\theta,\phi;\delta_n)\right] \\ w &= \frac{1}{2\mu}\mathrm{Re}\left[\sum_{\delta_n}\beta_n r^{\delta_n+1}\tilde{w}_n(\theta,\phi;\delta_n)\right] \end{aligned} \tag{2}$$

where (r, θ, ϕ) are the spherical coordinates with the origin at the vertex O, and (u, v, w) are the components of displacement in (r, θ, ϕ) directions, respectively. Values of δ_n are called the eigenvalues and their corresponding eigenfunctions are $\tilde{u}_n(\theta,\phi;\delta_n)$, $\tilde{v}_n(\theta,\phi;\delta_n)$ and $\tilde{w}_n(\theta,\phi;\delta_n)$. These displacement fields are required to satisfy the equilibrium equations within the conical region V, and the proper homogeneous boundary conditions on the lateral surface S_L. Note that the expression above is the generalization of the series expansion in terms of the spherical harmonics (Gurtin, 1972), just as the two-dimensional analogue (Im and Kim, 2000) is the generalization of the series solution in terms of the cylindrical harmonics.

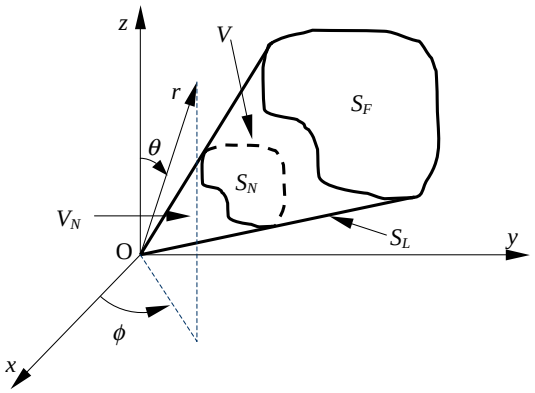

Fig. 1. The configuration at the three-dimensional generic conical vertex.

When the displacement fields are given by Eq. (2), the stress fields are expressed in the following form, proportional to r^{δ_n}:

$$\sigma_{ij} = \mathrm{Re}\left[\sum_{\delta_n} \beta_n r^{\delta_n} \tilde{\sigma}_{ij}(\theta, \phi, \delta_n)\right] \tag{3}$$

Hence, the stress singularity occurs at the origin when $\mathrm{Re}(\delta_n) < 0$. On the other hand, the strain energy is bounded at the origin and this requires $\mathrm{Re}(\delta_n) > -3/2$ (boundedness of strain energy requires $\mathrm{Re}(\delta_n) > -1$ for two-dimensional wedge vertices). However, $\mathrm{Re}(\delta_n) < -1$ implies that the displacement fields are unbounded at $r = 0$, which is unrealistic except for a concentrated load applied at the vertex. Therefore, we are primarily interested in eigenvalues δ_n in the range $-1 < \mathrm{Re}(\delta_n) < 0$.

Consider now a small subdomain V_N of the entire region V, as shown in Fig. 1 again. The subdomain V_N is the region enclosed by the vertex, the lateral surface S_L and the surface S_N, which is the concentric surface $r = r_N$. We choose the sufficiently small r_N so that the near-field expression (2) is valid in the subdomain V_N. Suppose we cut through the surface S_N to obtain V_N. Then the eigenfunction expansion for the displacement field (2) should satisfy the equilibrium equation inside the cone, the near-field boundary conditions on S_L and the appropriate traction condition on S_N. Therefore the principle of minimum potential energy is written as

$$\delta U - \int_{S_N} (t_r \delta u + t_\theta \delta v + t_\phi \delta w) r^2 \sin\theta \, \mathrm{d}\theta \, \mathrm{d}\phi = 0 \tag{4}$$

where

$$U = \int_{V_N} W r^2 \sin\theta \, \mathrm{d}r \, \mathrm{d}\theta \, \mathrm{d}\phi$$

is the total strain energy in the volume V_N of the cone, and W is the strain energy density, which is a function of the strains. The strain components are functions of the displacements and their first derivatives. The expression (4) of the principle of minimum potential energy is rewritten as (see Somaratna and Ting, 1986; Ghahremani, 1991 for detail):

$$\begin{aligned} &\int_{V_N} \left[\left\{ \psi_{,u} - \frac{\partial}{\partial r}(\psi_{,u_r}) \right\} \delta u + \psi_{,u_\theta} \delta u_\theta + \psi_{,u_\phi} \delta u_\phi + \left\{ \psi_{,v} - \frac{\partial}{\partial r}(\psi_{,v_r}) \right\} \delta v + \psi_{,v_\theta} \delta v_\theta + \psi_{,v_\phi} \delta v_\phi \right. \\ &\left. + \left\{ \psi_{,w} - \frac{\partial}{\partial r}(\psi_{,w_r}) \right\} \delta w + \psi_{,w_\theta} \delta w_\theta + \psi_{,w_\phi} \delta w_\phi \right] \mathrm{d}r \, \mathrm{d}\theta \, \mathrm{d}\phi = 0 \quad \text{and} \\ &\sigma_{rr} = t_r, \quad \sigma_{r\theta} = t_\theta, \quad \sigma_{r\phi} = t_\phi \quad \text{on } S_N \end{aligned} \tag{5}$$

where $\psi = W r^2 \sin\theta$ and the subscripts r, θ and ϕ in u, v and w denote the partial differentiation or the derivative of displacement like $u_r = \frac{\partial u}{\partial r}$. Furthermore, the comma after ψ indicates the partial differentiation with respect to the subject variable, for example, $\psi_{,u} = \frac{\partial \psi}{\partial u}$, and $\psi_{,u_r} = \frac{\partial \psi}{\partial u_r} = \frac{\partial \psi}{\partial (\partial u / \partial r)}$, etc. Since we assume that the traction on S_N is denoted by (t_r, t_θ, t_ϕ), we come to the conclusion that Eq. (5) is a variational statement that would ensure the satisfaction of the equations of equilibrium in V_N and the boundary conditions on S_L only.

The variational statement of Eq. (5) can be evaluated using the finite element method by discretizing the concentric spherical surface or the $\theta - \phi$ surface with an arbitrary constant value of r, say, $r = 1$ into finite elements. The nodal variables are chosen to be the spherical components of the eigenfunctions $\tilde{u}_n(\theta, \phi; \delta_n)$, $\tilde{v}_n(\theta, \phi; \delta_n)$ and $\tilde{w}_n(\theta, \phi; \delta_n)$ in Eq. (2). Details for discretizing the Eq. (5) are described in Somaratna and Ting (1986) and Ghahremani (1991). Thus finite element formulation of Eq. (5) leads to the following quadratic eigenvalue problem:

$$(\mathbf{K} + \delta_n \mathbf{D} + \delta_n^2 \mathbf{M})\mathbf{p} = 0 \tag{6}$$

where **K**, **D** and **M** are non-symmetric and square matrices and **p** is the eigenvector of the nodal displacements (see Somaratna and Ting, 1986; Ghahremani, 1991 for detail).

The eigenvalue problem for δ_n is quadratic, i.e., of the form $(\mathbf{K} + \delta_n \mathbf{D} + \delta_n^2 \mathbf{M})\mathbf{p} = 0$. We employ the inverse iterative method, which is very effectively applied for calculating an eigenvector (Bathe, 1995) together with the eigenvalue. We utilize the common scheme to convert the quadratic problem to a linear problem (Ghahremani, 1991) since the inverse iterative method is not directly applicable to the quadratic eigenvalue problems. The inverse iterative method yields the eigenvector corresponding to the smallest eigenvalue, and the origin of the δ_n-plane along the real axis should be shifted to obtain other eigenvalues. Moreover, by shifting the origin close to the desired eigenvalue, the convergence rate can be greatly improved (Bathe, 1995).

Finite element mesh consists of two-dimensional eight-node isoparametric quadrilateral elements. Numerical integration is performed using Gaussian quadrature rule on a grid of $n_G \times n_G$ integration points. In a general anisotropic material the material stiffness matrix C_{ij} is functions of θ and ϕ, and it will display a strong dependence on these terms. Note that the examination of expressions involved in Eq. (5) or (6) shows that terms like $1/\sin\theta$ also are present. Although terms like $1/\sin\theta$ occur because the strains are obtained in the spherical coordinate system, the integrand of Eq. (5) is not singular as Eq. (5) is derived from the principle of minimum potential energy. However, this leads to some difficulties numerically in evaluating the integrals accurately especially in the region near the pole of the coordinate system where $\theta \cong 0$. To avoid the numerical difficulties in evaluating the integral of Eq. (5) at the poles, we find the optimal number of integration points and the optimal mesh size by numerical testing (Somaratna and Ting, 1986).

3. Application of two-state *M*-integral to three-dimensional wedges

The M-integral is written as (Knowles and Sternberg, 1978):

$$M = \int_S \left\{ W x_i n_i - t_i u_{i,k} x_k + \frac{m-n}{m} t_i u_i \right\} \mathrm{d}S \tag{7}$$

where "S" is a closed surface. Note that W and t_i indicate the strain energy density and the traction components, given as $W = \frac{1}{2} C_{ijkl} \varepsilon_{ij} \varepsilon_{kl}$ and $t_i = \sigma_{ij} n_j$. Furthermore, u_i are the displacement components in rectangular coordinates. The constant m is the degree of homogeneity of the strain energy density, that is, 2 for the linear elastic problem and n is the degree of freedom of the spatial dimension, e.g., n equal to 2 for two-dimensional domains or to 3 for three-dimensional bodies. Thus the M-integral for three-dimensional linear elastic bodies is rewritten as

$$M = \int_S \left\{ W x_i n_i - t_i u_{i,j} x_j - \frac{1}{2} t_i u_i \right\} \mathrm{d}S \quad (i,j = 1,2,3)$$

Suppose two independent elastic states, "A" and "B". We consider another elastic state "C" obtained by superposing the two equilibrium states "A" and "B". Then the above M-integral is written as

$$M^{\mathrm{C}} = M^{\mathrm{A}} + M^{\mathrm{B}} + M^{(\mathrm{A,B})} \tag{8}$$

where the superscripts "A", "B" and "C" indicate the aforementioned elastic states, and $M^{(\mathrm{A,B})}$ is the two-state M-integral for three-dimensional domains, given as

$$M^{(\mathrm{A,B})} = \int_S \left[C_{ijkl} \varepsilon_{ij}^{\mathrm{A}} \varepsilon_{kl}^{\mathrm{B}} n_p x_p - (t_i^{\mathrm{A}} u_{i,p}^{\mathrm{B}} + t_i^{\mathrm{B}} u_{i,p}^{\mathrm{A}}) x_p - \frac{1}{2} (t_i^{\mathrm{A}} u_i^{\mathrm{B}} + t_i^{\mathrm{B}} u_i^{\mathrm{A}}) \right] \mathrm{d}S \tag{9}$$

The integral $M^{(A,B)}$ results from the mutual interaction between the two elastic states "A" and "B". This integral is referred to as the two-state M-integral in this context. Note that $M^{(A,B)}$ is the conservation integral for two equilibrium states since it identically vanishes for the domains with no singularities.

To explain the application of $M^{(A,B)}$ for generic three-dimensional wedges, we reconsider the conical domain in Fig. 2, where each of the two surfaces S_I and S_{II}, having the outward normal vectors, cuts through the lateral surface S_L in an arbitrary manner. Recalling that the M-integral is dependent upon the origin of the coordinate system (x_1, x_2, x_3), we take its origin at the wedge vertex. We take the closed surface $S_{II} - S_I + S_L$ where $-S_I$ means the reverse orientation of the surface S_I, that is, the same area but with the opposite normal vectors. With no singularities inside the region bounded by these surfaces, we can show the path independence of the M-integral as

$$M(S_I) = M(S_{II}) \tag{10}$$

where $M(S_L) = 0$ and $M(-S_I) = -M(S_I)$ have been used. Furthermore, the path or surface independence of the two-state M-integral $M^{(A,B)}$ is apparent from the above and Eq. (8). That is, we have

$$M^{(A,B)}(S_I) = M^{(A,B)}(S_{II}) \tag{11}$$

It is well known that the accurate computation of the two-state integral $M^{(A,B)}$ on the far field is possible only via a regular displacement based FEM in conjunction with the volume integral for three-dimensional domains (Li et al., 1985; Nikishkov and Atluri, 1987; Moran and Shih, 1987). Now utilizing the domain integral and going through some manipulation, we can reach the following expressions for three-dimensional bodies:

$$M^{(A,B)} = -\int_{V_{II}-V_I} \left[C_{ijkm}\varepsilon^A_{ij}\varepsilon^B_{km}x_l - (\sigma^A_{li}u^B_{i,j}x_j + \sigma^B_{li}u^A_{i,j}x_j) - \frac{1}{2}(\sigma^A_{li}u^B_i + \sigma^B_{li}u^A_i) \right] q_{,l}\,\mathrm{d}V \tag{12}$$

where V_I and V_{II} represent the domains bounded by S_I and S_L, and S_{II} and S_L, respectively, and V_{II}–V_I indicates the region bounded by S_{II} and S_I in Fig. 2. The function $q(x_1, x_2, x_3)$ is a weight function that is defined as 1 on S_I and as 0 on S_{II} with smooth variation between S_I and S_{II}. Note that the expression (10) and (11) indicate that M and $M^{(A,B)}$ are conserved for an arbitrary banded volume V_{II}–V_I.

We are now at the stage of applying the aforementioned two-state M-integral for finding the free constant β_l in the eigenfunction series Eq. (2). Let β_s denote the free constant for the singular stress, which is the

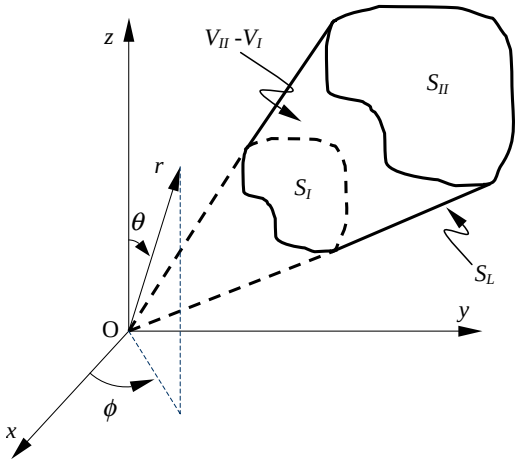

Fig. 2. The integral path for M-integral and two-state M-integral for three-dimensional wedges.

first term in Eqs. (2) and (3). In the numerical examples to follow in the next section, we will focus on this term as it represents the near-tip intensity of the singular stress field under a proper normalization of the eigenfunction. However, the present scheme is equally applicable for finding any higher order eigenfunction term as well, and so we explain the scheme for an arbitrary free constant β_l.

The key idea of calculating β_l is to utilize the path or surface independence property of $M^{(A,B)}$, as given in Eq. (11). Firstly, a convenient auxiliary state "B" is chosen, and the elastic field of the wedge under consideration is assigned to "A". $M^{(A,B)}(S_I)$ is then calculated semi-analytically on the $\theta - \phi$ domain with $r = 1$ of the spherical coordinates. We need numerical integration to evaluate the resulting integral on this domain. Next, from finite element analysis we obtain $M^{(A,B)}(S_{II})$ on the right hand side of Eq. (11) with the aid of the volume integral expression (12). Then Eq. (11) yields β_l and this value must be invariant with respect to the choice of the auxiliary elastic state as $M^{(A,B)}$ is a bilinear functional of the two elastic states "A" and "B".

The present procedure now boils downs to the choice of a convenient auxiliary state "B". For this we define a complementary eigenfield for a given eigenstate. Let the complementary eigenvalue δ_l^c of an arbitrary eigenvalue δ_l be defined in the M-integral sense as follows (Lee and Im, 2003):

$$\delta_l + \delta_l^c = -3 \tag{13}$$

This may be compared with its two-dimensional analogue (Im and Kim, 2000; Jeon and Im, 2001; Lee et al., 2001), given as

$$\delta_l + \delta_l^c = -2$$

As will be verified later, δ_l^c constitutes another eigenvalue as long as δ_l belongs to the eigenvalues for a given problem. Benthem (1980) discussed the fact that $-\delta_l - 3$ is also an eigenvalue if δ_l is the vertex singularity of a quarter infinite crack. In general this is true for every eigenvalue and for generic three-dimensional wedges wherein the M-integral is conserved. We showed numerically this for a quarter infinite crack and a bimaterial interface corner in another paper (Lee and Im, 2003) and will numerically verify for the given numerical example in this paper.

Suppose we are interested in finding a free constant β_l. Then, for the auxiliary state we take the elastic state of the complementary eigenvalue δ_l^c, which is written as

$$\begin{aligned} u^c &= \frac{1}{2\mu}\mathrm{Re}\left[\beta_l^c r^{\delta_l^c+1}\tilde{u}_l^c(\theta,\phi,\delta_l^c)\right] \\ v^c &= \frac{1}{2\mu}\mathrm{Re}\left[\beta_l^c r^{\delta_l^c+1}\tilde{v}_l^c(\theta,\phi,\delta_l^c)\right] \\ w^c &= \frac{1}{2\mu}\mathrm{Re}\left[\beta_l^c r^{\delta_l^c+1}\tilde{w}_l^c(\theta,\phi,\delta_l^c)\right] \end{aligned} \tag{14}$$

where the intensity β_l^c of the complementary eigenfield is prescribed arbitrarily. To calculate $M^{(A,B)}(S_I)$ in Eq. (11) we substitute the elastic field (2) for the elastic state "A", and the complementary elastic field (14) for the elastic state "B". Then, the following expression is obtained for the two-state integral $M^{(A,B)}(S_I)$ after some algebra (see Lee and Im, 2003 for detail):

$$M^{(A,B)}(S_I) = \sum_{\delta_n}\int_S \mathrm{Re}\left[\beta_n\beta_l^c r^{\delta_n+\delta_l^c+3}G(\delta_n,\delta_l^c) + \beta_n\bar{\beta}_l^c r^{\delta_n+\bar{\delta}_l^c+3}G(\delta_n,\bar{\delta}_l^c)\right]\mathrm{d}\theta\,\mathrm{d}\phi \tag{15}$$

where $G(\delta_n,\delta_l^c)$ is given by Lee and Im (2003). Note that we take the summation sign outside the integral symbol by exploiting firstly the path or surface independence property and secondly the fact that each individual eigenfunction term in the series expansion (2) is a separate elastic state satisfying the governing equations and the near-field boundary conditions on S_L in Fig. 1.

For Eq. (11) with Eq. (15) to be valid, the surface S_I of $M^{(A,B)}(S_I)$ on the left hand side of Eq. (11) should be located sufficiently close to the vertex O because the expression (2), which has been substituted to obtain Eq. (15), is legitimate near the vertex. However, in actuality the path or surface independence property of the two-state M-integral makes $M^{(A,B)}(S_I)$ invariant with respect to the radial coordinate r. This is apparent if S_I is chosen to be a concentric surface with the radial distance, say $\hat{r}$ from the vertex. If $\delta_n + \delta_l^c > -3$, we take $\hat{r}$ to go to zero so that the M-integral contribution from δ_n may be shown to be zero. On the other hand, we choose $\hat{r}$ to be an infinitely large value in order to show that the M-integral contribution disappears for $\delta_n + \delta_l^c < -3$ as well. The only non-vanishing contribution originates from the case $\delta_n + \delta_l^c = -3$, and all the other terms disappear, so that $M^{(A,B)}(S_I)$ has no $\hat{r}$ dependence and that the expression (15) involves the integration merely on the $\theta - \phi$ domain. This implies that the only non-zero contribution to $M^{(A,B)}(S_I)$ occurs from $\delta_n = -3 - \delta_l^c = \delta_l$, that is, from the complementary pair of eigenvalues. This property is shown to hold for the two-state J- and M-integral in two-dimensional cases. The right hand side $M^{(A,B)}(S_{II})$ is now calculated from finite element analysis with the aid of the domain integral representation (12). Then Eq. (11) will yield the free constant β_l, and so the near-tip stress intensity β_s of the singular field if δ_s is chosen for δ_l.

4. Numerical example: a laminated composite with a transverse crack

For our numerical example, we choose a laminated composite with a transverse crack at the free surface as shown in Fig. 3. Somaratna and Ting (1986) first computed the stress singularities of this example and later Ghahremani (1991) verified their results. Somaratna and Ting (1986) considered that each layer is composed of the same material although the ply angle α of the layers may be different in Fig. 3. The material is T300/5208 graphite/epoxy, which is orthotropic. The material properties in the material principal frame are given as (Somaratna and Ting, 1986):

$$E_1 = E_2 = 22\ \text{GPa}, \quad E_3 = 319\ \text{GPa}$$
$$G_{12} = G_{23} = G_{31} = 11.7\ \text{GPa}$$
$$v_{21} = v_{31} = v_{32} = 0.28$$

where E_i is Young's moduli, G_{ij} is shear moduli and v_{ij} is Poisson's ratio. The orientation of the material axis is specified with the aid of the ply angle α as shown in Fig. 3. We take this example firstly to compare the stress singularities with other results, and next to compute the near-tip intensity or free constant β_s with the aid of the two-state M-integral. In this work, we choose a cross ply composite, of which the ply angle α_1 is

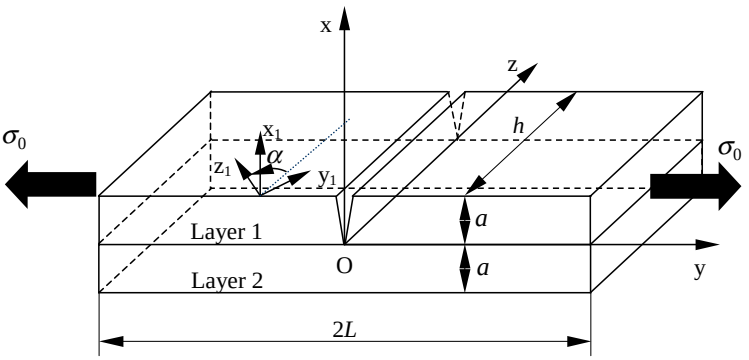

Fig. 3. The geometric configuration of a laminated composite with a transverse crack.

equal to 0° for the upper layer and the ply angle α_2 equal to 90° for the lower layer, where α_1 and α_2 are the counterclockwise orientation of fibers from the z-axis.

At a point sufficiently close to a three-dimensional crack corner the asymptotic solutions should be characterized by the solutions of a quarter infinite crack in a half-space (Nakamura and Parks, 1988; Nakamura and Parks, 1989). The eigenvalues in the present case are obtained for the vertex of a quarter infinite crack as shown in Fig. 4. The domain is considered in the half-space, $z \geqslant 0$ and the crack front is along the z-axis. To compute the eigenvalues for a quarter infinite crack, we consider the surface on the unit sphere onto the $\theta - \phi$ plane with $r = 1$ as shown in Fig. 4 and discretize this domain for finite element analysis utilizing the eight-node plane element. We take the half model to compute the eigenvalues and impose symmetric boundary conditions on the plane of symmetry $\phi = \pi$ and traction free conditions on other boundaries. The domain with $0 \leqslant \theta \leqslant \pi/2$ and $0 \leqslant \phi \leqslant \pi$ has the interface of two the layers at $\phi = \pi/2$. The domain was subdivided into $n_\theta \times n_\phi$ elements: n_θ is the number of elements in the θ-direction and n_ϕ the number of elements in the ϕ-direction. Used are the 8×16 mesh with eight-node element and 5×5 Gaussian integration points per element. Table 1 shows that the eigenvalues satisfy the complementarity relationship $\delta_l + \delta_l^c = -3$ in the three-dimensional M-integral sense. We compare the stress singularity with the result obtained by Ghahremani (1991) in Table 1. The two values of the stress singularity for a [0/90] laminated composite are in good agreement.

Recall that the three-dimensional crack corner as shown in Fig. 3 has a singularity line of the crack front as well as the vertex of the crack front line intersecting with the free surfaces. Since we consider a laminated composite with a transverse crack, the solutions contain also the edge singularity along the crack front line. While the edge singularity of the three-dimensional crack corner is the well-known inverse square root singularity, the edge singularity of a laminated composite with a transverse crack varies according to the angle of the transverse crack. When the direction of the transverse crack is perpendicular to the interface of two layers as shown in Fig. 3, there are two edge singularities, which are real. Note that Lee and Im (2003) adopted the singular element along the crack front line to deal the inverse square root singularity of three-dimensional crack corner. However, we do not utilize the singular element but the regular element along the crack front line, since the singular element represents only the inverse square root singularity.

To apply the two-state M-integral to a laminated composite with a transverse crack, we cannot directly utilize the integral path (or surface) for the two-state M-integral as shown in Fig. 2 because a singularity line exists along the crack front line like the three-dimensional crack corner (see Fig. 4). The contribution

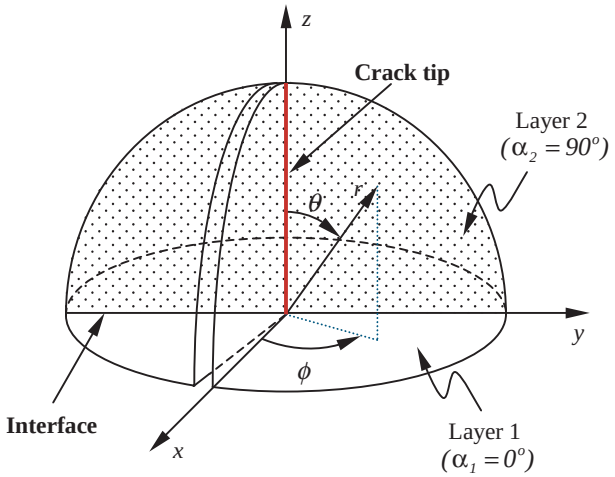

Fig. 4. The domain for computing the stress singularity near the vertex of a transverse crack in a laminated composite.

Table 1
Complementary pairs of eigenvalues of a laminated composite with a transverse crack ($\delta_n + \delta_n^c = -3$)

Eigenvalue
−3.0006
−3.0001
−3.0000
−2.6579
−2.4502
−2.0005
−2.0002
−2.0000
−1.0000
−0.9998
−0.9995
−0.5498
−0.3422
0.0000
0.0001
0.0006

of two-state M-integral calculated on the surface along the crack front line as shown in Fig. 5 is expressed as (Lee and Im, 2003):

$$M^{(\mathrm{A,B})}(S_\mathrm{t}) = \lim_{\rho\to 0}\int_{S_\mathrm{t}} \left\{ W^{(\mathrm{A,B})}\rho - t_i^{\mathrm{A}}\frac{\partial u_i^{\mathrm{B}}}{\partial \rho}\rho - t_i^{\mathrm{A}}\frac{\partial u_i^{\mathrm{B}}}{\partial z}z - t_i^{\mathrm{B}}\frac{\partial u_i^{\mathrm{A}}}{\partial \rho}\rho - t_i^{\mathrm{B}}\frac{\partial u_i^{\mathrm{A}}}{\partial z}z - \frac{1}{2}t_i^{\mathrm{A}}u_i^{\mathrm{B}} - \frac{1}{2}t_i^{\mathrm{B}}u_i^{\mathrm{A}} \right\}\rho\,\mathrm{d}z\,\mathrm{d}\varphi \tag{16}$$

where S_t indicates the integral path shown in Figs. 5 and 6. Note that the tube S_t does not include the singular vertex point ($r = 0$), and that the two elastic states "A" and "B" have the edge singularity $\delta_\mathrm{s}^\mathrm{e}(-1 < \delta_\mathrm{s}^\mathrm{e} < 0)$ along the crack front line $z > 0$. Taking into account the fact that $\frac{\partial u_i^{\mathrm{B}}}{\partial z}$ and $\frac{\partial u_i^{\mathrm{A}}}{\partial z}$ are not

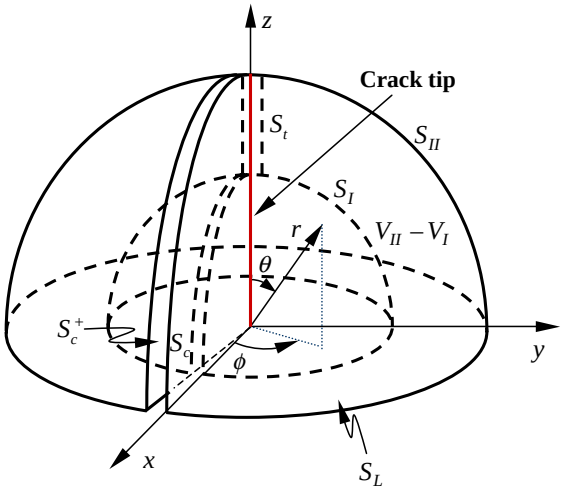

Fig. 5. The modified integral path $S_\mathrm{II} - S_\mathrm{t} + S_\mathrm{c}^+ + S_\mathrm{c}^- - S_\mathrm{I} + S_\mathrm{L}$ of the two-state M-integral for the three-dimensional crack corner.

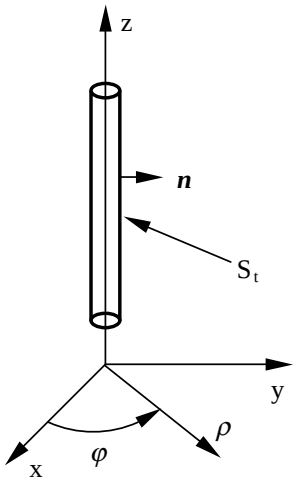

Fig. 6. The integral path of the two-state M-integral for the three-dimensional crack corner along the crack front line.

singular along the crack front line $z > 0$, we see that Eq. (16) goes to zero at the rate of $O(\rho^{2(1+\delta_s^e)})$ as ρ approaches zero. Therefore, we can ignore the contribution of two-state M-integral calculated on the surface along the crack front line.

We consider a laminated composite of cross ply [0/90] under remote tension. Thus we take the half model using the symmetry. The finite element mesh with 4800 twenty-node solid elements (the number of DOF $\sim$ 67,000) and the boundary conditions for the symmetric deformation are shown in Fig. 7. The finite element mesh near the crack vertex is refined due to the presence of the three-dimensional singularity. Finite element analysis has been carried out using the package code ABAQUS.

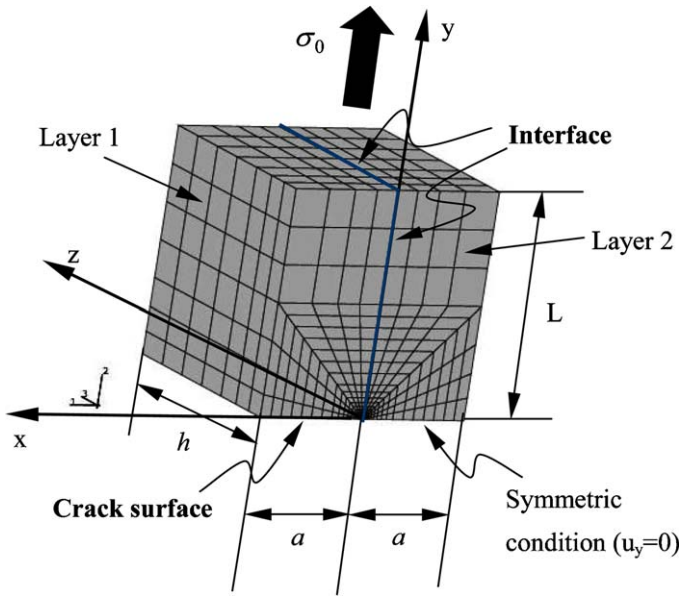

Fig. 7. The half finite element model of the [0/90] laminated composite with a transverse crack.

Table 2
The stress singularity δ_s and the free constant β_s for the transverse crack in a [0/90] laminate composite

	Stress singularity δ_s	Free constant β_s
Ghahremani's result	−0.3420	–
The present result	−0.3422	2.4614×10^{-6}

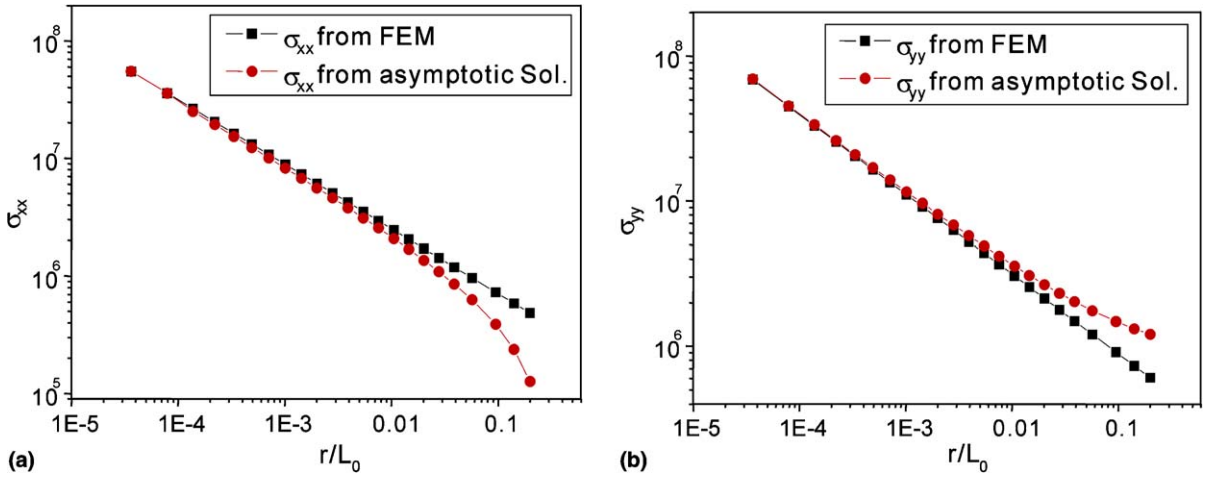

Fig. 8. The comparison of the asymptotic solutions with the finite results along the ligament surface ($\theta = \pi/2$, $\phi = \pi$), (a) σ_{xx}; (b) σ_{yy}.

The free constant β_s is obtained via the two-state M-integral. Note that the value of the free constant β_s is dependent upon the way that the eigenfunction $(\tilde{u}, \tilde{v}, \tilde{w})$ are normalized. For this example, we choose to normalize the eigenfunctions such that the maximum magnitude of the three spherical components $\tilde{u}$, $\tilde{v}$ and $\tilde{w}$ may become 1. Using the free constant β_s in Table 2, we compute stresses from the asymptotic solution and compare it with the results from the finite element analysis along the line $\theta = \pi/2$ and $\phi = \pi$ in Fig. 8. The finite element solution is in a good agreement with the asymptotic solution including only the singular term in vertex region as shown in Fig. 8.

5. Conclusions

We have examined the singular stress field around the tip of a transverse crack at which the transverse crack meets with free surface in a laminated composite. Moreover, we compute the singular stress states near the three-dimensional vertices in this anisotropic body with the aid of the two-state M-integral and the eigenfuntion expansion. We verify numerically that the eigenvalues of the present three-dimensional problems satisfy the complementarity relationship, $\delta_n + \delta_n^c = -3$, in the three-dimensional M-integral sense. This relationship and the surface independence of the two-state M-integral are applied for extracting the near-tip intensity of the singular stress fields for the three-dimensional tip of the transverse crack in the present laminated composite. The numerical example demonstrates that the present scheme is effective for computing the intensities of singular stresses near the generic three-dimensional anisotropic wedges in a laminated composite.

References

Bathe, K., 1995. Finite Element Procedures. Prentice-Hall International, USA.

Bazant, Z.P., Estenssoro, L.F., 1979. Surface singularity and crack propagation. International Journal of Solids and Structures 15, 405–426.

Benthem, J.P., 1977. State of stress at the vertex of a quarter-infinite crack in a half-space. International Journal of Solids and Structures 13, 479–492.

Benthem, J.P., 1980. The quarter-infinite crack in a half-space; alternative and additional solutions. International Journal of Solids and Structures 16, 119–130.

Ghahremani, F., 1991. A numerical variational method for extracting 3D singularities. International Journal of Solids and Structures 27, 1371–1386.

Gurtin, M.E., 1972. The linear theory of elasticityHandbuch der Physik. Springer-Verlag.

Im, S., Kim, K.S., 2000. Application of the two-state *M*-integral for computing an intensity of singular near-tip field for a generic composite wedge. Journal of the Mechanics and Physics in Solids 48, 129–151.

Jeon, I., Im, S., 2001. The role of higher order eigenfields in elastic–plastic cracks. Journal of the Mechanics and Physics in Solids 49, 2789–2818.

Kim, Y.J., Kim, H.G., Im, S., 2001. Mode decomposition of three-dimensional mixed mode cracks via two-state integral. International Journal of Solids and Structures 38, 6405–6426.

Knowles, J.K., Sternberg, E., 1978. On a class of conservation laws in a linearized and finite elatostatics. Archive for Rational Mechanics and Analysis 44, 187–211.

Koguchi, H., Muramoto, T., 2000. The order of stress singularity near the vertex in three dimensional joints. International Journal of Solids and Structures 37, 4737–4762.

Labossiere, P.E.W., Dunn, M.L., 2001. Fracture initiation at three-dimensional bimaterial interface corners. Journal of the Mechanics and Physics in Solids 49, 609–634.

Lee, Y., Im, S., 2003. On the computation of the near-tip stress intensity for three-dimensional wedges via two-state *M*-integral. Journal of the Mechanics and Physics in Solids 51, 825–850.

Lee, Y., Goo, N.S., Im, S., 2001. Application of two-state *M*-integral for analysis of adhesive lap joints. International Journal for Numerical Methods in Engineering 52, 903–920.

Li, F.Z., Shih, F.C., Needleman, A., 1985. A comparison of methods for calculating energy release rates. Engineering Fracture Mechanics 21, 405–421.

Moran, B., Shih, C.F., 1987. Crack tip and associated domain integral from momentum and energy balance. Engineering Fracture Mechanics 27, 615–642.

Nakamura, T., Parks, D.M., 1988. Three-dimensional stress field near the crack front of a thin elastic plate. ASME Journal of Applied Mechanics 55, 805–813.

Nakamura, T., Parks, D.M., 1989. Antisymmetrical 3-D stress field near the crack front of a thin elastic plate. International Journal of Solids and Structures 25, 1411–1426.

Nikishkov, G.P., Atluri, S.N., 1987. An equivalent domain integral method for computing crack tip integral parameters in nonelastic, thermo-mechanical fracture. Engineering Fracture Mechanics 26, 851–867.

Picu, C.R., Gupta, V., 1997. Three-dimensional stress singularities at the tip of a grain triple junction line intersecting the free surface. Journal of the Mechanics and Physics in Solids 45, 1495–1520.

Somaratna, N., Ting, T.C.T., 1986. Three-dimensional stress singularities in anisotropic materials and composites. International Journal of Engineering Science 24, 1115–1134.